

A RIEMANNIAN-GEOMETRICAL MODEL OF SIMULTANEOUS CONTRAST ILLUSIONS AND THE FIGURAL AFTER-EFFECTS ON THE BASIS OF DEPTH EFFECTS

Toshimasa Yamazaki* and Takahiro Yamanoi**

A study was undertaken to construct a descriptive model of both simultaneous contrast illusions and the figural after-effects in terms of a Riemannian space with Riemann-Christoffel curvature tensor. This differential-geometrical model was applied to the illusion of concentric circles (the Delboeuf illusion), the figural after-effect and the *benl line* illusion (the Orbison square illusion).

The curvature tensor $R_{\lambda\mu\nu}$, which can be calculated from the metric tensor specifying the perceived distortion in these illusions, implies another distortion effect which cannot be described within two-dimensional plane (*depth effect*). This effect occurs in any figural after-effects, while the simultaneous contrast and the figural after-effect only for small inspection time does not evoke this effect. Therefore, the later phenomenon can be formulated by $R_{\lambda\mu\nu} = 0$, and the former by $R_{\lambda\mu\nu} \neq 0$. Assuming that an indicatrix is elliptic in the local perceptual field of parallel lines and solving $R_{\lambda\mu\nu} = 0$ uniquely determined the magnitudes of the illusions as a fractional function in which a parameter is involved. The sign of the parameter was decisive of whether the simultaneous illusion or the figural after-effect with small inspection time is evoked. Moreover, extending the present model to the summation of the effect of each circle led us to simulate a *visually straight* line in the Orbison square illusion.

1. Introduction

Vision is a process of inference (Hoffman, 1983). This process implies that location, orientation, size and color of visual information passing through the retina and the LGN (Lateral Geniculate Nucleus) would be detected in the visual cortices, and such attributes be used to recognize patterns and objects in the higher cortices. Various geometrical-optical illusions and the associated figural after-effects, which are always easy to observe remarkably, reveal spatio-temporal aspects of such visual information processing mechanisms.

Enormous theories have been proposed over the last 200 years to explain these phenomena. According to Gillam (1980), the theories fell into four categories:

Key Words and Phrases: Riemannian geometry, simultaneous contrast illusions, figural after-effects, depth effects, Riemann-Christoffel curvature tensor, indicatrix, Delboeuf illusion, Orbison illusion

* Fundamental Research Laboratories, NEC Corporation, 34 Miyukigaoka, Tsukuba, Ibaraki, 305-8501 Japan

** Division of Electronics and Information Engineering, Faculty of Engineering, Hokkai Gakuen University, S26-jo, W11-chome, Chuo-ku, Sapporo, 064-0926 Japan

† Requests for reprints should be sent to: Dr. Toshimasa Yamazaki, Fundamental Research Laboratories, NEC Corporation, 34 Miyukigaoka, Tsukuba, Ibaraki, 305-8501 Japan (TEL: +81 (298) 50-1124; FAX: +81 (298) 56-6136; E-mail address: yamazaki@frl.el.nec.co.jp)

classification theories, *activity theories* (e.g. Nowakowska, 1983), *physiological theories* and *functional theories*. Many of the *physiological theories* or *neural confusion theories* are based on lateral inhibition at the retinal level (e.g. Ganz, 1966; Walker, 1973) and at the cortical level (e.g. Blakemore et al., 1970; Oyama, 1977). The controversy between retinal theories and cortical ones (MacLeod et al., 1974; Walker, 1974) could not be resolved without consideration of more subtle, higher-order effects. The *functional theories* (e.g. Gregory, 1968) have been developed on the basis of an assumption that many geometrical-optical illusions could be related to cues to the size of objects in the three-dimensional world. Gregory's perspective theory (1968) must introduce unconsciously perceived depth. In the words of Humphrey and Morgan (1965), "A theory which appeals to the idea of automatic compensation for unconsciously perceived depth is in obvious danger of being irrefutable." Such a function related with depth perception, however, might be considered as one of the candidates for the higher-order effects.

The present study will focus on mathematical theories, especially differential-geometrical approaches to both the geometrical-optical illusions and the figural after-effects. Such approaches are *descriptive* in terms of difficulty in finding physiological substance of mathematical formulations for these phenomena. Nevertheless, it had been already proved in many other phenomenon, for example, binocular visual space perception (Luneburg, 1947; Indow, 1974, 1979, 1982; Eschenburg, 1980; Yamazaki, 1987), color space (Brown & MacAdam, 1949; Von Schelling, 1956; Jain, 1972), color perception (Resnikoff, 1974), shape perception (Caelli, 1977), apparent motion (Foster, 1975), motion perception (Caelli et al., 1978) and so on, that a differential geometry is one of the most powerful tools for treating with visual perception.

Differential-geometrical approaches to visual illusions (Hoffman, 1971; Smith, 1978; Kawabata, 1976; Watson, 1978; Yamanoi et al., 1981) have the advantage that the existing illusions can be quantitatively described by the model simulations and new phenomena could be predicted and produced without psychological experiments. In Hoffman's model (1971), Lie transformation groups correspond to visual constancies such as shape constancy and size constancy. In Smith's model (1978), apparent curves in geometrical-optical illusions are attributed to a first-order differential equation which is mathematically equivalent to Hoffman's Lie-theoretic model. Kawabata (1976) first introduced geodesics into the *perceptual field* in the sense that these lines give a minimum distance between any two points, calculated strengths of the perceptual field for the Müller-Lyer, the Poggendorff and the Zöllner figures and explained these illusions as distortions of the metric of the field. Watson (1978) and Yamanoi et al. (1981) introduced a Riemannian metric into the differential-geometrical theory on the basis of *force field* produced by lines. Yamanoi et al. (1981) exemplified *visually straight* lines, which are defined as geodesics in the Riemannian space, in the Orbison illusion and the Hering illusion. However, they only calculated the curvature tensor but did not refer to the phenom-

enal meaning. Similarly, Watson (1978) obtained the solutions for the equations of the geodesics for the Enclosure illusion, the Müller-Lyer illusion, the Ponzo illusion and the figural after-effects. It seems very difficult for only the metric properties of Riemannian spaces to account for the Delboeuf illusion and the figural after-effect, because the geodesic is responsible for only the illusions associated with length and straightness.

The motivation for this study is to relate the curvature tensor in a Riemannian space with depth perception which could reflect the higher-order effects (e.g. Hubel & Livingstone, 1987; Saito et al., 1986; Toyama & Kozasa, 1982) than those in the retina and the primary visual cortex. The reason is that Köhler and Wallach (1944, p. 275) observed that the test figure is perceived not only to become smaller but also to *lay back in space*. This phenomenon implies displacement effects which could not be described within two-dimensional flat plane where visual stimuli are presented. In order to account for the effect, the visual field under the present theory is assumed to have not only the metric tensor but also explicitly the curvature tensor in connection with the stimulus field.

An outline of the present model is as follows: The visual field, as contrasted with stimulus fields, is modeled with a Riemannian space. The perceived distortion will specify the metric. The Riemann-Christoffel curvature tensor R_{AB} , which can be calculated from the metric, implies another distortion effect which cannot be described within two-dimensional flat plane. This effect occurs in figural after-effects, while the simultaneous contrast between figures does not evoke this effect. Therefore, the latter phenomenon can be formulated by $R_{AB} = 0$, and the former by $R_{AB} \neq 0$. By solving these equations, this model could simulate quantitatively the magnitudes of displacement effects in both the geometrical-optical illusions and the figural after-effects. These visual illusions are illustrated in Fig. 1.

In Section 2, within a general framework of differential geometry various geometrical quantities such as the metric tensor, the coefficients of connection and the curvature tensor, are introduced into the local perceptual field. Especially, the bent line illusion is defined by the equation of geodesic, and the curvature tensor implies the depth effects in the figural after-effects. Assuming that an indicatrix is elliptic in the perceptual field of parallel lines and solving an equation formulated by no depth effect uniquely determine the magnitudes of the illusion of concentric circles, of the figural after-effects and of the transition process from the simultaneous illusion to the figural after-effect in Sections 3, 4 and 5, respectively. Section 6 generalizes the present model to the Orbison square illusion.

¹ Hereafter we call *depth effect*, and

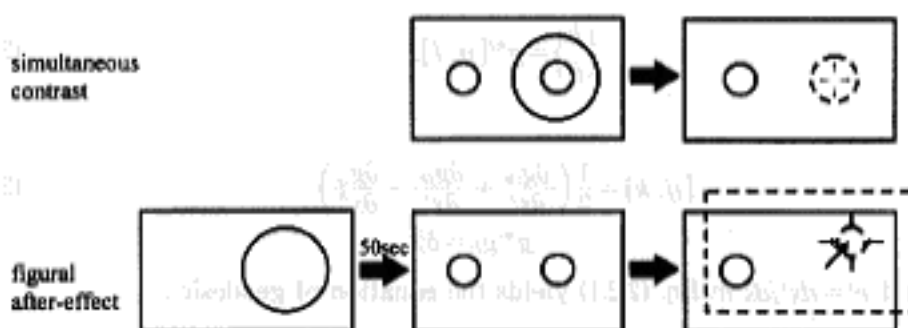


Fig. 1.1 Schema of three effects which the present study will address itself to. Displacement effects on concentric circles in the simultaneous contrast and in the figural after-effect (overestimation of inner circles and underestimation of the inner circles, respectively) and also *depth effect* occurred in the latter situation, which will be formulated in Section 2.3 and discussed in Sections 6 and 8.

2. Differential-geometrical framework for simultaneous contrast illusions and the figural after-effects

2.1 Metrics

Assuming that the stimulus field such as a two-dimensional flat plane be a two-dimensional spatial continuum, each point in the stimulus field is represented by the spatial coordinates x^i ($i=1, 2$). Between line-elements dx^i ($i=1, 2$) composing the stimulus field where figures such as circles and lines are presented, and line-elements $(dx)^a$ ($a=1, 2$) which the perceived stimulus field consists of, a locally defined linear relation

$$(dx)^a = A_i^a dx^i, \quad dx^i = A_a^i (dx)^a \quad (2.1.1)$$

is assumed, where the transformation tensor A_i^a and its inverse A_a^i are functions of point x^b ($b=1, 2$), and Einstein's summation is adopted throughout this paper with respect to repeated indices. Moreover, the length ds of line element dx^i is given by

$$ds^2 = \delta_{ab} (dx)^a (dx)^b = \delta_{ab} A_i^a A_j^b dx^i dx^j,$$

and the metric tensor can be written as

$$g_{ij} = \delta_{ab} A_i^a A_j^b,$$


where δ_{ab} is Kronecker's delta.

2.2 Parallelism and geodesic

According to Levi-Civita (1917), the parallelism of a vector $v^i(t)$ on a curve $x^i = x^i(t)$ (t is a parameter) in a Riemannian space with g_{ij} , is defined as that the covariant derivative of v^i is zero, that is,

$$\frac{\delta v^i}{\delta t} = \frac{dv^i}{dt} + \left\{ \begin{matrix} i \\ kj \end{matrix} \right\} v^j \frac{dx^k}{dt} = 0. \quad (2.2.1)$$

Note that $\left\{ \begin{matrix} i \\ kj \end{matrix} \right\}$ are called the Christoffel symbols of the second kind, and are given by

where  $\begin{Bmatrix} k \\ ij \end{Bmatrix} = g^{kl} [ij, l],$ (2.2.2)

$[ij, k] = \frac{1}{2} \left(\frac{\partial g_{ik}}{\partial x^j} + \frac{\partial g_{jk}}{\partial x^i} - \frac{\partial g_{ij}}{\partial x^k} \right)$ (2.2.3)
 $g^{kl} g_{lj} = \delta_j^k,$
 $t = s$ and $v' = dx'/ds$ in Eq. (2.2.1) yields the equation of geodesic:

$$\frac{\partial}{\partial s} \left(\frac{dx^i}{ds} \right) = \frac{d^2 x^i}{ds^2} + \begin{Bmatrix} i \\ hj \end{Bmatrix} \frac{dx^h}{ds} \frac{dx^j}{ds} = 0,$$

where s depicts the arc length. The geodesic is a generalization of a straight line in Euclidean space, and corresponds to a reconstruction in physical space that would be perceived to be *straight*, and *vice versa*. This concept has been related with *bent line* illusions such as the Hering illusion and the Orbison square illusion. Yamanoi et al. (1981) explained these illusions by numerical solutions of the geodesics. Watson (1976) also described quantitatively the Enclosure, the Müller-Lyer and the Ponzo illusions in terms of the geodesics.

2.3 Phenomenal meaning of Riemann-Christoffel curvature tensor

There is one more important geometrical quantity, curvature tensor, in a Riemannian space, in addition to metric tensor and the Christoffel symbols. This section will address itself to phenomenal meaning of the curvature tensor.

Given a metric g_{ij} , a distortion tensor e_{ij} defined by

$$e_{ij} = \frac{1}{2} (\delta_{ij} - g_{ij})$$

describes the state of perceived distortion, where δ_{ij} is Kronecker's delta. This tensor e_{ij} could be given by the symmetrical part of an ordinary deformation tensor ϵ_{ij} . For example, this tensor is defined by

$$\frac{1}{2} (\epsilon_{ij} + \epsilon_{ji}) = \frac{1}{2} \left(\frac{\partial u_i}{\partial x^j} + \frac{\partial u_j}{\partial x^i} \right), \quad \frac{1}{2} (\epsilon_{ij} - \epsilon_{ji}) = \frac{1}{2} \left(\frac{\partial u_i}{\partial x^j} - \frac{\partial u_j}{\partial x^i} \right) + \omega_{ij},$$

where u_i is a displacement vector, and ω_{ij} is a rotation independent of that on the basis of the displacement $((\partial u_i / \partial x^j - \partial u_j / \partial x^i) / 2)$.

By the compatibility condition for the distortion tensor e_{ij} , the integrability condition of the equation

$$\frac{1}{2} \left(\frac{\partial u_i}{\partial x^j} + \frac{\partial u_j}{\partial x^i} \right) = e_{ij} \tag{2.3.1}$$

reduces to

$$R_{hijl} = 0.$$

Here, the R_{hijl} is called the Riemann-Christoffel curvature tensor, and is given by

$$R_{hij} = \frac{\partial[il, h]}{\partial x^j} - \frac{\partial[ij, h]}{\partial x^l} + [hl, a] \left\{ \frac{a}{ij} \right\} - [hj, a] \left\{ \frac{a}{il} \right\}. \quad (2.3.2)$$

The curvature tensor R_{hij} implies the ordinary incompatibility. That is, if $R_{hij} \neq 0$, then the integrability condition of Eq. (2.3.1) is not assured. This implies a (three-dimensional) distortion effect which cannot be described within two-dimensional plane surface. On the other hand, $R_{hij} = 0$ guarantees that geometrical-optical illusions evoke two-dimensional displacement effect.

3. Application to the Delboeuf illusion

3.1 Formulations for the illusion of concentric circles

Metric properties could be obtained by specifying an indicatrix³⁾ in any perceptual field. The perceptual field of concentric circles may be locally regarded as those of parallel lines. The indicatrix in the field of parallel lines had been experimentally proved to be elliptic (Yamanoi et al., 1982) as follows:

$$(X^1)^2 + \phi^2(X^2)^2 = 1, \quad (3.1.1)$$

where local coordinates X^i are introduced into the neighborhood of (x^1, x^2) so that X^2 refers to the tangent direction of circles and X^1 the orthogonal to X^2 , that is,

$$X^1 = dx^1 \cos \alpha + dx^2 \sin \alpha, \quad X^2 = -dx^1 \sin \alpha + dx^2 \cos \alpha \quad (3.1.2)$$

(see Fig. 3.1.1). This results not only demonstrates a deformation along the parallel lines but also guarantees that the metric is not Euclidean but Riemannian. The function ϕ represents the effects of the field of one circle (stimulus circle; SC), and would be determined as the magnitudes of illusion in case of the concentric circles later. At the present time, we suppose only that the magnitudes be isotropic, that is, the functions of only a distance from the origin (Fig. 3.1.1):

$$\phi = \phi(r),$$

while Yamanoi et al. (1981) had given this function ϕ in advance. Then, for the derivation of the metric tensor, we can use the following lemma (Laugwitz, 1965, p. 178):

Lemma 3.1 Given the indicatrix $f(x^i, dx^i) = 0$, the metric tensor is given by

$$g_{ij} = \frac{1}{2} \frac{\partial^2 L^2}{\partial y^i \partial y^j} \quad (y^i = dx^i), \quad (3.1.3)$$

³⁾When in a metric space a distance between two points P and Q is defined by $L(Q-P)$, and $L(X)$ is nonzero and homogeneous, meets the triangle inequality and is continuous and sufficiently differentiable, the hypersurface

$$L(X) = 1$$

is called the *indicatrix* (Laugwitz, 1965, p. 179). In case of a two-dimensional Euclidean space, the *indicatrix* corresponds to a unit circle.

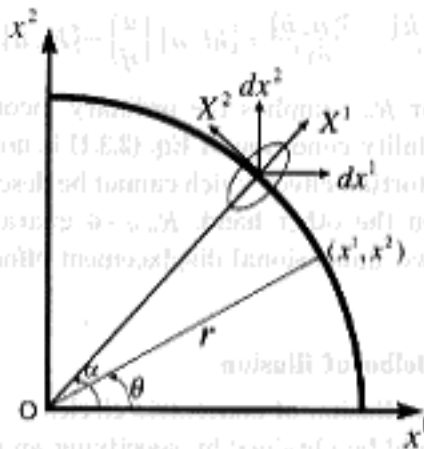


Fig. 3.1.1 Relationship between global coordinates x^i and local coordinates X^i

where the metric base function L is obtained by solving $f(x^i, dx^i/L) = 0$.

From $L^2 = (X^1)^2 + \phi^2(X^2)^2$, Eqs. (3.1.2) and (3.1.3), we have

$$g_{ij} = \begin{pmatrix} \phi^2 - \psi(x^1)^2 & -\psi x^1 x^2 \\ -\psi x^1 x^2 & \phi^2 - \psi(x^2)^2 \end{pmatrix} \quad (i, j = 1, 2), \quad (3.1.4)$$

where

$$\psi \equiv \frac{\phi^2 - 1}{r^2}, \quad r^2 = (x^1)^2 + (x^2)^2. \quad (3.1.5)$$

Equation (3.1.4) means that this metric is Riemannian, because of independence from dx^i ($i = 1, 2$). Moreover, using this metric, the perceived size of a circle with a radius r_1 in the field is proved to be

$$\begin{aligned} \int_{r=r_1} ds &= \int_{r=r_1} \sqrt{g_{ij} dx^i dx^j} \\ &= \int_0^{2\pi} \sqrt{g_{ij} \frac{dx^i}{d\theta} \frac{dx^j}{d\theta}} d\theta \\ &= \int_0^{2\pi} r_1 \phi d\theta \\ &= 2\pi r_1 \phi \end{aligned} \quad (3.1.6)$$

for any position $(x^1, x^2) = (r_1 \cos \theta, r_1 \sin \theta)$ on the TC (see Fig. 3.1.1).

In a two-dimensional Riemannian space, the number of essential components of the curvature tensor is only one. From Eqs. (2.3.2)-(2.3.4), (3.1.4) and (3.1.5) we obtain

$$R_{1212} = \phi(\phi'' + \frac{2}{r}\phi'). \quad (3.1.7)$$

where ' depicts the ordinary derivative with respect to r . By setting $R_{2112} = 0$, we can derive an equation with respect to ϕ :

$$\phi'' + \frac{2}{r} \phi' = 0, \quad (3.1.8)$$

whose solutions are given by

$$\phi(r) = -\frac{C_1}{r} + C_2, \quad (3.1.9)$$

where C_1 and C_2 are arbitrary constants.

3.2. Experiment on the Delboeuf illusion

In order to compare the model simulation with the psychological data, the authors carried out an experiment on the illusion of concentric circles (Yamazaki, 1990; Yamanoi, 1998).

3.2.1 Apparatus

A subject, whose head is fixed by a chin rest, watches a CRT display with binocularity throughout this experiment. The distance from the subject's eyes to a screen of the CRT display is 100 cm. The stimulus configuration on the screen is as shown in Fig. 3.2.1.1. On the screen there are concentrically a test circle (TC) and a stimulus circle (SC) on the right side with respect to a gazing point marked "x" and a comparison circle (CC) on the left side. The stimulus conditions are composed of a series of inner circles (TCs), whose diameters are 15, 20 and 25 mm (0.86°, 1.14° and 1.43°, respectively, in visual angles), surrounded by the SC with a diameter of 30 mm (1.72° in visual angle), and a series of outer circles (TCs), whose diameters are 40, 50 and 60 mm (2.28°, 2.86° and 3.42°, respectively, in visual angles), surrounding the SC. This experiment was throughout made in a room with dim light.

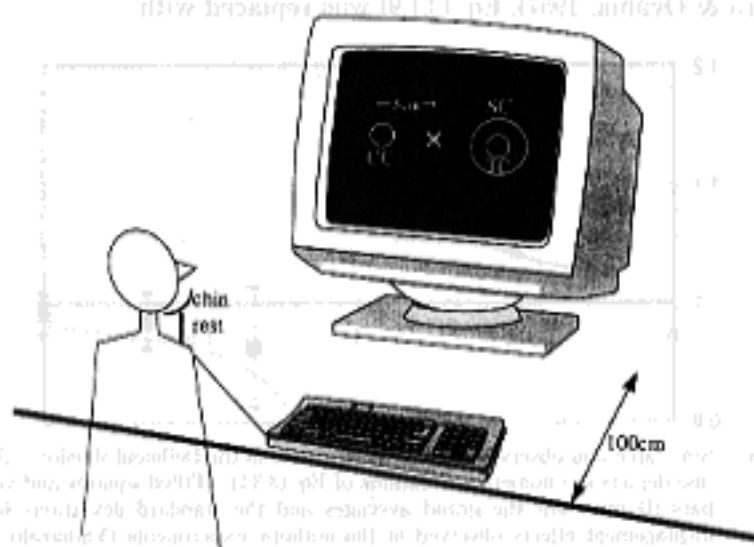


Fig. 3.2.1.1 The Delboeuf illusion experiment (Yamazaki, 1990; Yamanoi, 1998). The experimental situation and the stimulus configuration.

3.2.2 Subjects

Twelve subjects, which consisted of 2-female and 4-male university students and 6-male graduate students at the age of 21-26, participated this experiment. Each subject had normal or corrected-to-normal vision.

3.2.3 Procedure

The subject is requested to report a difference in size between the TC and the CC by the method of three categories. All the report was carried out by the keyboard input. The PSE (point of subjective equality) is determined by the method of limits where one ascending series and one descending series are involved and the CC's diameter varies at an interval of 1 mm. These procedures were controlled by a personal computer (NEC PC9801E or NEC PC9801VX). The magnitude of the illusion was defined as the difference in PSE between the TC and the control condition where there is only the SC.

3.2.4 Results

In Fig. 3.3.1 filled squares and vertical bars (I) depict the grand averages and the standard deviations, respectively, of the magnitudes as a function of the ratio of the size of the TC to that of the SC. As seen from this figure, a tendency was observed that inner circles are over-estimated and outer circles under-estimated, as well as the results of Ogasawara (1952).

3.3 Model simulations

Under the rough condition that the magnitude of the illusion is a fractional function with respect to r according to Eq. (3.1.9), many simulations were tried for the data fitting. These results showed $C_2 \approx 1$. On the basis of this finding and that the magnitude is a function of the size ratio of the TC to the SC (e.g. Ogasawara, 1952; Sagara & Oyama, 1957), Eq. (3.1.9) was replaced with

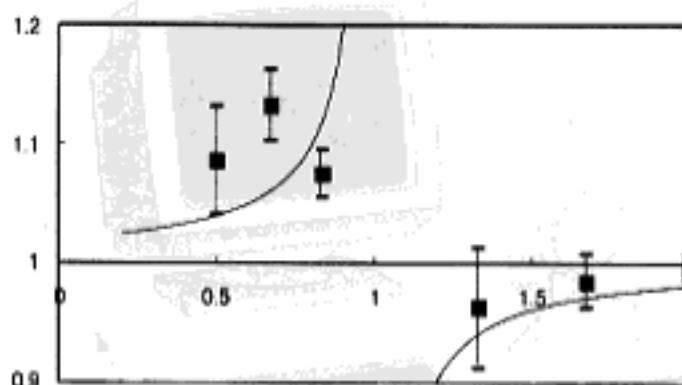


Fig. 3.3.1 Simulated and observed displacement effects in the Delboeuf illusion. A solid line depicts the numerical solutions of Eq. (3.3.1). Filled squares and vertical bars (I) represent the grand averages and the standard deviations for the displacement effects observed at the authors' experiments (Yamazaki, 1990; Yamanoi, 1998). The abscissa represents the ratio of the radius of the test circle (TC) to that of the stimulus circle (SC). The ordinate (in mm) is defined by the difference in PSE between the TC and the control condition.

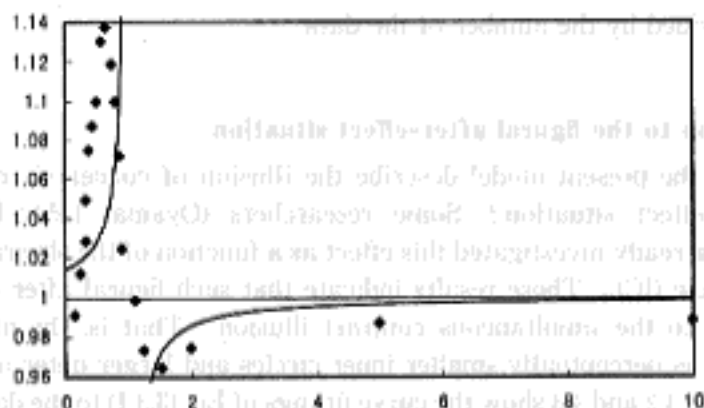


Fig. 3.3.2 Simulated and observed displacement effects in the Delboeuf illusion. A solid line depicts the numerical solutions of Eq. (3.3.1). Filled diamonds represent Ogasawara's results (Ogasawara, 1952, p. 225, Table 3. (a)III; p. 228, Table 5. (a)III; p. 229, Table 7. (a)IV) for the TC of 40 mm in diameter. The abscissa and the ordinate are the same in Fig. 3.3.1.

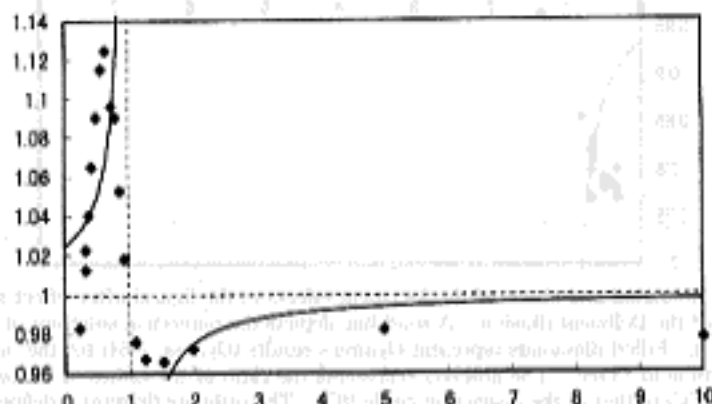


Fig. 3.3.3 Simulated and observed displacement effects in the Delboeuf illusion. A solid line depicts the numerical solutions of Eq. (3.3.1). Filled diamonds represent Ogasawara's results (Ogasawara, 1952, p. 225, Table 3. (a)III; p. 228, Table 5. (a)III; p. 229, Table 7(a)) for the TC of 60 mm in diameter. The abscissa and the ordinate are the same in Fig. 3.3.1.

$$\phi(\bar{r}) = -\frac{C_1}{\bar{r}-1} + 1 \quad \left(\bar{r} = \frac{r}{r_1} \right) \quad (3.3.1)$$

where r_1 represents the radius of the SC. Then, the corrected function was fitted to both the psychological data obtained in the previous section and that of Ogasawara (1952).

Solid lines in Figs. 3.3.1, 3.3.2 and 3.3.3 show the results on the curve fittings to the data of the present study and the data of Ogasawara for the TCs of 40 mm and 60 mm in diameters (2.5° and 3.8° in visual angles) (Ogasawara 1952, Table 3(a) p. 225, Table 5(a) p. 228, Table 7(a) p. 229), respectively. These figures demonstrate a rough approximation of Eq. (3.3.1). Note that "Error" in Table 1 is defined by the sum of squares of the differences between the psychological data and the model

simulation divided by the number of the data.

4. Application to the figural after-effect situation

How can the present model describe the illusion of concentric circles in the figural after-effect situation? Some researchers (Oyama, 1954; Ikeda, 1951; Kogiso) have already investigated this effect as a function of the size ratio of TC to inspection circle (IC). These results indicate that such figural after-effect is perfectly reverse to the simultaneous contrast illusion. That is, the after-effect is characterized as perceptually smaller inner circles and larger outer ones.

Figures 4.1, 4.2 and 4.3 show the curve fittings of Eq. (3.3.1) to the data of Oyama

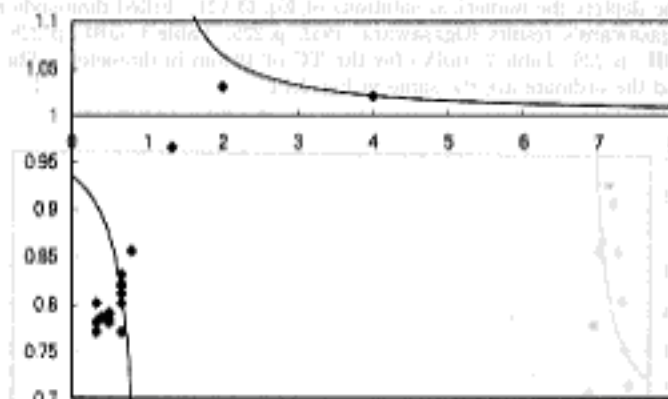


Fig. 4.1 Simulated and observed displacement effects in the figural after-effect situation of the Delboeuf illusion. A solid line depicts the numerical solutions of Eq. (3.3.1). Filled diamonds represent Oyama's results (Oyama, 1954) for the inspection time of 15 sec. The abscissa represents the ratio of the radius of the test circle (TC) to that of the inspection circle (IC). The ordinate (in mm) is defined by the difference in PSE between the TC and the control condition.

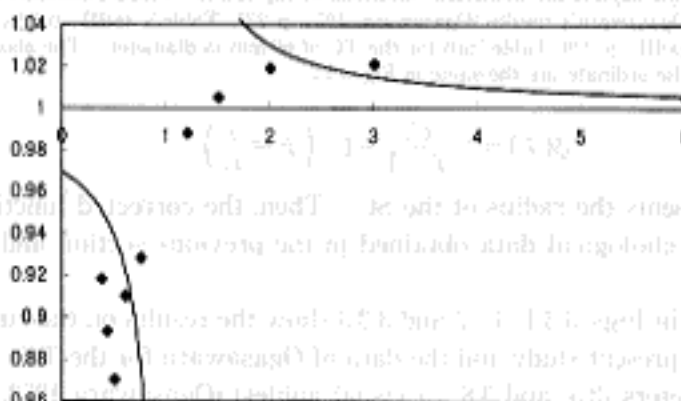


Fig. 4.2 Simulated and observed displacement effects in the figural after-effect situation of the Delboeuf illusion. A solid line depicts the numerical solutions of Eq. (3.3.1). Filled diamonds represent Ikeda's results (Ikeda, 1951) for the inspection time of 120 sec. The abscissa and the ordinate are the same in Fig. 4.1.

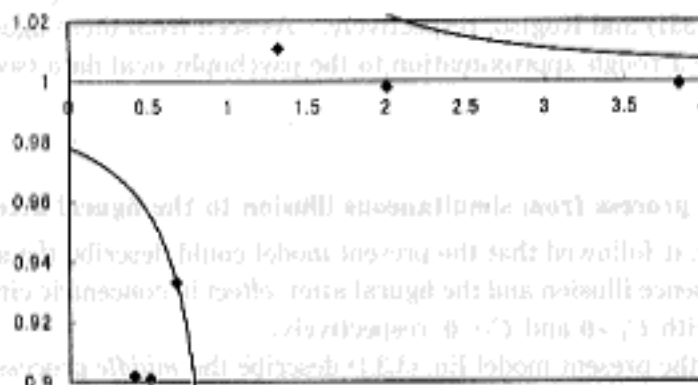


Fig. 4.3 Simulated and observed displacement effects in the figural after-effect situation of the Delboeuf illusion. A solid line depicts the numerical solutions of Eq. (3.3.1). Filled diamonds represent Kogiso's results (Kogiso) for the inspection time of 15 sec. These points were directly taken from Kogiso's data mentioned in Oyama (1956, p. 30). The abscissa and the ordinate are the same in Fig. 4.1.

Table 1
Data Used in Curve Fittings and Estimated Parameters

Source	C_1	Error	Inspection Time (s)	SOA (msec)	Remarks
Yamazaki (1990) & Yamanol (1998)	0.01980	0.00013	0	0	TC=0.86~3.42
Ogasawara (1952)	0.01428	0.00321	0	0	TC=2.5
	0.02495	0.00129	0	0	TC=3.8
Oyama (1964)	-0.06421	0.00687	15	0	
Ikeda (1951)	-0.03046	0.00164	120	0	
Kogiso (Oyama, 1956)	-0.02210	0.00181	15	0	
Ikeda & Obonai (1955)	0.00604	0.00073	0.5	0	TC=1.72
	0.00532	0.00024	0.5	20	IC=0.58~4.58
	0.00388	0.00025	0.5	60	
	0.00025	0.00025	0.5	100	
	-0.00334	0.00016	0.5	200	
	-0.00716	0.00030	0.5	300	
	-0.00644	0.00039	0.5	400	
	-0.01133	0.00042	0.5	440	
	-0.01169	0.00043	0.5	460	
	-0.01259	0.00057	0.5	480	
	-0.01460	0.00061	0.5	500	
	-0.01604	0.00064	0.5	520	
	-0.01676	0.00078	0.5	540	
	-0.01931	0.00089	0.5	560	
	-0.01676	0.00078	0.5	600	
	-0.01532	0.00068	0.5	700	
	-0.01327	0.00035	0.5	800	
	-0.01018	0.00025	0.5	1,000	

(1954), Ikeda (1951) and Kogiso, respectively. As seen from these figures, $C_1 < 0$ in Eq. (3.3.1) gave a rough approximation to the psychophysical data (see also Table 1).

5. Transition process from simultaneous illusion to the figural after-effect

Untill now, it followed that the present model could describe the simultaneous contrast-confluence illusion and the figural after-effect in concentric circle situation as Eq. (3.3.1) with $C_1 > 0$ and $C_1 < 0$, respectively.

Then, can the present model Eq. (3.3.1) describe the *middle* process, that is, the transition process from the simultaneous illusion to the figural after-effect in terms of inspection time? Ikeda and Obonai (1955) investigated effects of exposure delay with inspection time fixed (500 msec) on this process.

5.1 Experiment by Ikeda and Obonai

The above researchers investigated the transition process from the simultaneous illusion of concentric circles to the figural after-effects in terms of exposure delay. Their experiment is summarized as follows:

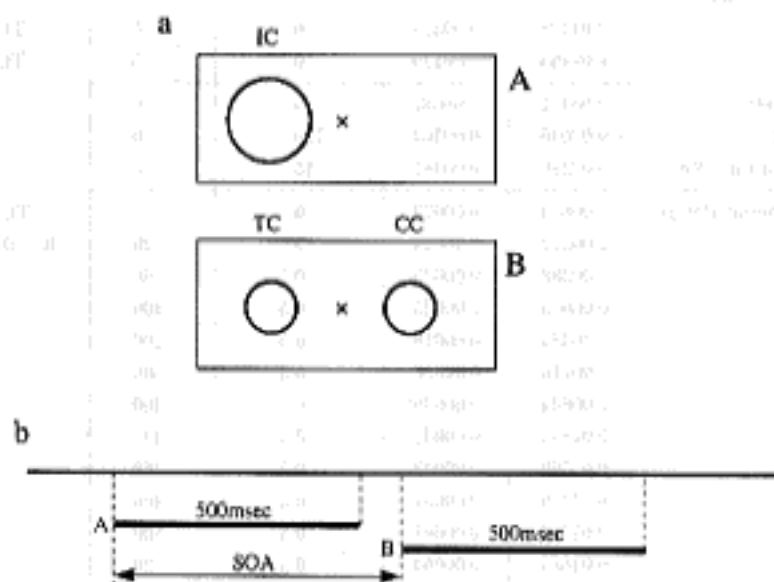


Fig. 5.1.1.1 Ikeda and Obonai's experiment (1955) on the transition process from the simultaneous contrast to the figural after-effect in concentric circles. (a) Stimulus condition. Two panels A and B could be presented in the same visual field being overlapped. The panel A has an inspection circle (IC), the panel B has a test circle (TC) and a comparison circle (CC), and both panels a gazing point marked by "x". (b) Time scheduling of the stimulus condition. The duration time of the panels A and B is 500 msec. Ikeda and Obonai investigated the effect of SOA (stimulus onset asynchrony) between the two panels on the perceived size of the TC.

5.1.1 Apparatus

Two panels A and B were represented by a tachistoscope according to the time scheduling as shown in Fig. 5.1.1.b. The two panels could be located in the same position of the stimulus field being overlapped as to the time scheduling. The panel A had an IC, and the panel B a TC and a CC, where the CC was used to determine the perceived size of the TC, as shown in Fig. 5.1.1.a. There were seven different ICs whose diameters were 10, 15, 20, 30, 40, 60 and 80 mm. The diameter of TC was fixed at 30 mm, while that of CC varied from 22 mm to 36 mm with 1 mm steps. In order to investigate the transition process from the simultaneous illusion to the figural after-effects, eighteen SOAs (stimulus onset asynchronies) between the two panels were prepared during 0-1,000 msec. The duration time of each panel was constant at 500 msec. The brightness of stimulus fields was 60 lux. The distance from the subject's eyes to the stimulus field was one meter.

5.1.2 Subjects

Five college students in the psychology course participated in this experiment.

5.1.3 Procedure

The subjects were asked to judge whether CC was larger, smaller than or equal to TC. Six judgments were obtained for each pair of TC and CC under every SOA condition. The PSE was calculated on the basis of Wirth's formula in the method of constant stimuli.

5.1.4 Results

Figure 5.1.4.1 includes six graphs showing displacement effects for the SOA of

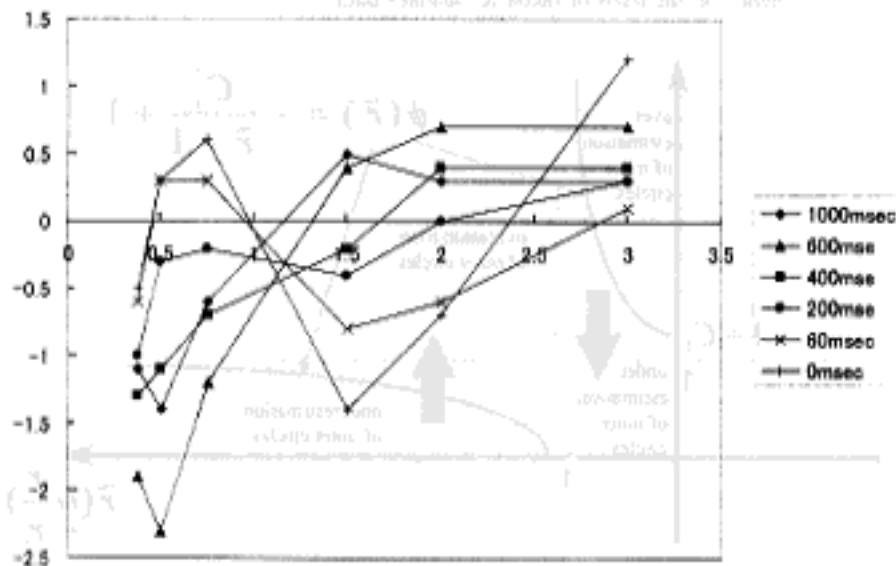


Fig. 5.1.4.1. Ikeda and Obonai's results (1955). Six graphs show the displacement effects for the SOA of 0, 60, 200, 400, 600, and 1,000 msec, respectively. The abscissa represents the ratio of the radius of the test circle (TC) to that of the inspection circle (IC). The ordinate (in mm) is defined by the difference in PSE between the TC and the control condition.

0, 60, 200, 400, 600 and 1,000 msec, respectively. From these data, it was observed that the increase of SOA results in the transition from overestimation of inner circles and underestimation of outer circles to underestimation of inner circles and overestimation of outer circles.

5.2 Application to Ikeda and Obonal's data

The current model was applied to the results in the previous section. The curve fittings of Eq. (3.3.1) to these data were summarized in Table 1 and Fig. 5.2.1.

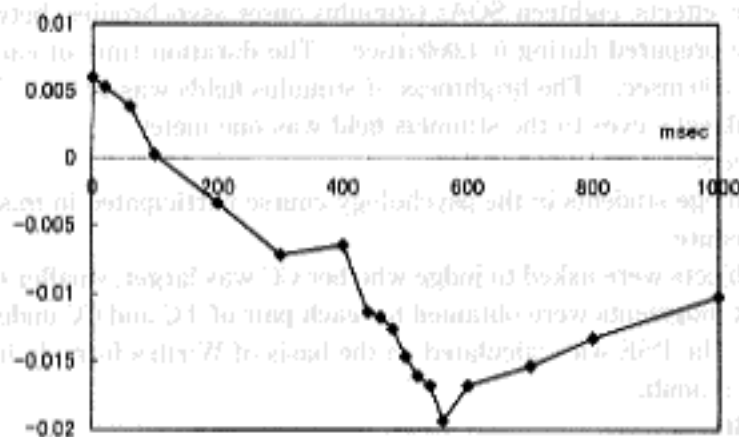
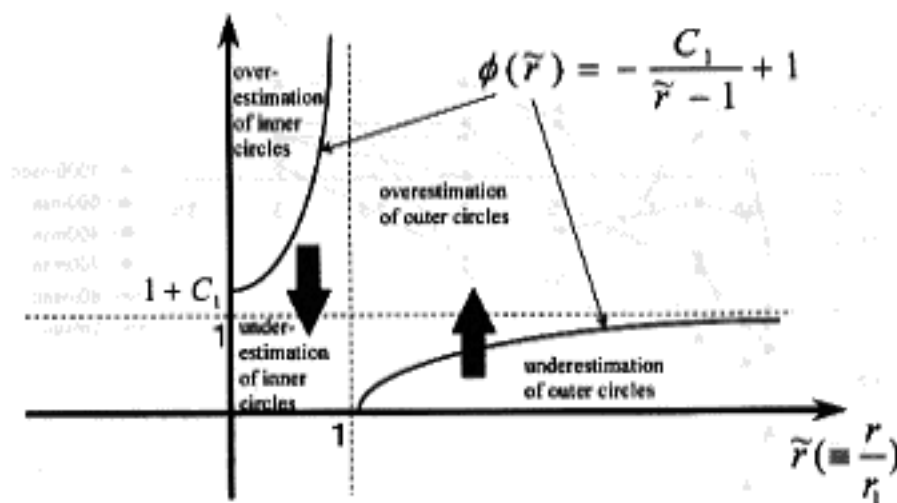


Fig. 5.2.1 Transition process from the simultaneous illusion to the figural after-effects as a function C_1 , which is the parameter included in Eq. (3.3.1), of the exposure delay, on the basis of Ikeda & Obonal's data.



➡ Transition Process from Simultaneous Illusions to Figural After-Effects

Fig. 5.2.2 Summary of the Delboeuf illusion; the figural after-effects and the transition process which are described by $C_1 > 0$, $C_1 < 0$ and $C_1 > 0 \rightarrow C_1 < 0$, respectively, in Eq. (3.3.1).

Especially, Fig. 5.2.1 indicates that the transition process from the simultaneous illusion to the figural after-effect can be described by the continuous variation of the sign of C_1 from plus to minus. However, we observe this temporal transition as only a function of the exposure delay but not of the inspection time. Figure 5.2.2 summarizes the present model involving the illusion of concentric circles, the figural after-effect and the transition process. These three kinds of spatio-temporal features for concentric circle situation can be described by $C_1 > 0$, $C_1 < 0$ and $C_1 > 0 \rightarrow C_1 < 0$, respectively, in Eq. (3.3.1).

6. Inspection time to evoke depth effect

How much of the inspection time does it take to evoke this *depth effect* certainly? The inspection time was four minutes in the experiment of Köhler and Wallach (1944). Figure 7.1 shows the relationship between the depth effect and the inspection time in the concentric circle situation. This result is based on the following experiment (Yamazaki, 1991): An IC was presented on the left side or the right one with respect to a fixation point marked by "×". Two test circles on both sides immediately followed the end of exposure of the IC. The duration of the exposure was 10, 30, 60, 90, 120 or 150 sec. The diameters of the IC and the TC were constant at 40 mm and 20 mm, respectively. Consequently, there were 12 different conditions of spatio-temporal arrangement. The distance from the fixation point to the center of each circle was 40 mm. The distance from a subject's eyes to the presentation plane was 47 cm. This experiment was throughout made in a dark

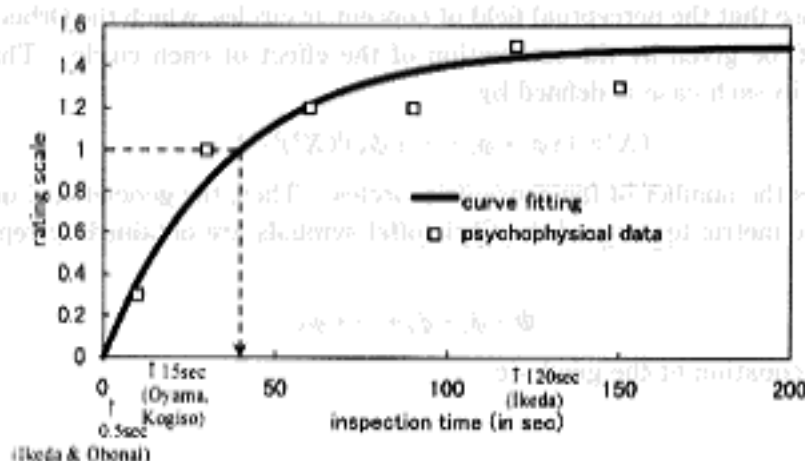


Fig. 6.1 *Depth effect* as a function of the exposure time of inspection circles. A rating scale of the ordinate is as follows: 0: cannot judge which test circle is farther away; 1: test circle on the left (or right) side is perceived to be slightly farther away than that on the right (or left) side; 2: farther away than on the right (or left) side. A solid line shows a function of Eq. (6.1) estimated from the psychological data. The *slightly farther away* requires an inspection time of more than 40 sec. The inspection times of Oyama (1954), Ikeda (1951), Kogiso and Ikeda and Obonai (1955) are also indicated in this figure.

room. The subject was requested to judge which test circle was farther away with binocularity. A rating scale for judgment was as follows: 2: test circle on the left (or right) side is perceived to be farther away than that on the right (or left) side; 1: slightly farther away; 0: cannot judge which circle is farther away. The time for the judgments was about 10 sec. In Fig. 6.1, the means for the rating scale are depicted by open squares. These data were fitted to a function of the inspection time t

$$d(t) = a(1 - e^{-bt}), \quad (6.1)$$

where a and b are constants³⁾, under the initial condition $d(0) = 0$ which implies that there is surely no *depth effect* in the simultaneous illusion. The linear least squares estimation yielded $a = 1.50205$ and $b = 0.02758$. In Fig. 6.1, the estimated function $d(t)$ is also depicted by a solid line. Being perceived to be slightly farther away requires an inspection time of more than 40 sec⁴⁾ on the basis of Eq. (6.1). Therefore, all the psychophysical experiments analyzed in the present study except for Ikeda's data (1951) would not have yielded any *depth effect*. This is why the present model within a framework of no *depth effect* could describe both the simultaneous illusion and the figural after-effect with small inspection time in the concentric circle situation.

7. Generalization to the Orbison square illusion

In this section, the present model will be extended to the illusion in the concentric circle field, that is, the Orbison square illusion (Orbison, 1939).

Suppose that the perceptual field of concentric circles, which the Orbison figure consists of, be given by the summation of the effect of each circle. That is, an indicatrix in such case is defined by

$$(X^1)^2 + (\phi_1 + \phi_2 + \dots + \phi_N)(X^2)^2 = 1, \quad (7.1)$$

where N is the number of the concentric circles. Then, the geometrical quantities such as the metric tensor and the Christoffel symbols are obtained by replacing ϕ with

$$\Phi \equiv \phi_1 + \phi_2 + \dots + \phi_N.$$

Thus, the equation of the geodesic

³⁾ Such exponential function had been applied to the psychological data concerning the figural after-effects (e.g. Hammer, 1949; Oyama, 1953). Especially, this function is in good agreement with the data having the *plateau* (e.g. Ichikawa, 1982) as the present data does.

⁴⁾ From Eq. (7.1), when $d(t) = 1$, t becomes

$$t = \frac{1}{b} \log \left(1 + \frac{1}{a} \right) \\ = 39.7 \approx 40 \text{ (sec).}$$

$$\frac{d^2 x^k}{ds^2} + \left\{ \begin{matrix} k \\ ij \end{matrix} \right\} \frac{dx^i}{ds} \frac{dx^j}{ds} = 0 \quad (i, j, k=1, 2) \quad (7.2)$$

with

$$\left\{ \begin{matrix} k \\ ij \end{matrix} \right\} = (\Phi D^* - \Psi^*) \delta_{ij} x^k - \frac{D^*}{\Phi} (\delta_{ik} x^j + \delta_{jk} x^i) - \left(M^* + \frac{2D^* \Psi^*}{\Phi} \right) x^i x^j x^k \quad (7.3)$$

should be a curve which would be perceived to be *straight* in the Orbison illusion, where

$$\Psi^* = \frac{\Phi^2 - 1}{r^2}, \quad D^* = -\frac{\Phi'}{r}, \quad M^* = -\frac{\Phi D^* + \Psi^*}{r^2}.$$

In order to examine this generalization, the authors carried out the following simulation. For the perceptual field of five concentric circles whose radii are 5, 10, 15, 20 and 25 mm, we solved numerically the equation of geodesic given by Eq. (7.2) with

$$\Phi = \phi_1 + \phi_2 + \phi_3 + \phi_4 + \phi_5,$$

and

$$\phi_1 = -\frac{C}{r-r_1}, \quad \phi_2 = -\frac{C}{r-r_2}, \quad \phi_3 = -\frac{C}{r-r_3}, \quad \phi_4 = -\frac{C}{r-r_4}, \quad \phi_5 = -\frac{C}{r-r_5},$$

where r_i ($i=1, \dots, 5$) are the radii of the five concentric circles, and C is a constant.

Under the transformation of the variables

$$y_1 = x^1, \quad y_2 = x^2, \quad y_3 = \frac{dx^1}{ds}, \quad y_4 = \frac{dx^2}{ds},$$

Eq. (6.2) is replaced by

$$\frac{dy_1}{ds} = y_3,$$

$$\frac{dy_2}{ds} = y_4,$$

$$\frac{dy_3}{ds} = -\left[\begin{matrix} 1 \\ 11 \end{matrix} \right] (y_3)^2 + 2 \begin{matrix} 1 \\ 12 \end{matrix} y_3 y_4 + \begin{matrix} 1 \\ 22 \end{matrix} (y_4)^2,$$

$$\frac{dy_4}{ds} = -\left[\begin{matrix} 2 \\ 11 \end{matrix} \right] (y_3)^2 + 2 \begin{matrix} 2 \\ 12 \end{matrix} y_3 y_4 + \begin{matrix} 2 \\ 22 \end{matrix} (y_4)^2,$$

which is a system of ordinary differential equations of the first order with four unknowns. The Runge-Kutta-Gill method is applied to this system. In a Riemannian space, the length of line-element ds is defined by

$$ds^2 = g_{ij} dx^i dx^j,$$

which can be written to

$$1 = g_{ij} \frac{dx^i}{ds} \frac{dx^j}{ds}.$$

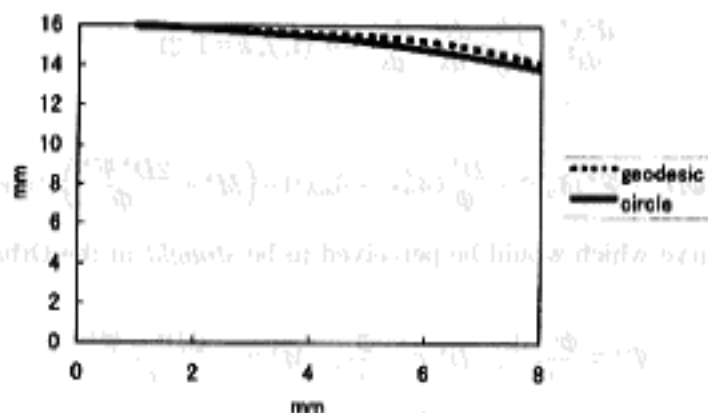


Fig. 7.1 An illustrative solution of the geodesic defined by Eqs. (7.2) and (7.3) in five concentric circles. A dotted line depicts the numerical solutions. A solid line represents one of the concentric circles, which could be compared with the obtained geodesic.

Therefore, at each process where numerical solutions are obtained in order, we replace y_3 and y_4 by y_3/T and y_4/T , respectively, where T is defined by

$$T = \sqrt{g_{13}(y_3)^2 + 2g_{12}y_3y_4 + g_{22}(y_4)^2}$$

for y_3 and y_4 given.

Figure 7.1 shows a result on this simulation. A dotted line depicts the numerical solutions of Eq. (7.2) under the initial condition $x^1=1.0$ (mm), $x^2=15.0$ (mm), $dx^1/ds=1.0$, $dx^2/ds=0.0$ and $s=0.0$. A solid line represents one of the concentric circles, which can be compared with the obtained geodesic. The slightly upper curve than this "circle" line would be perceived to be *straight* in the concentric circles.

8. Considerations and possible improvement

The authors proposed a descriptive model of both geometrical-optical illusions and the figural after-effects in terms of a Riemannian space with the curvature tensor which will lead us to predict *depth effects*. The phenomena had been reported by Köhler and Wallach (1944).

The present model including the Riemann-Christoffel curvature tensor is based on the following consideration: Consider an n -dimensional Riemannian space imbedded in an N -dimensional Euclidean space ($n < N$). Given the Cartesian coordinate X^a in the Euclidean space and the coordinate x^k in the subspace, the covariant differential of the Jacobian $B_k^a (= \partial X^a / \partial x^k)$ with respect to x^k

$$H_k^c = \frac{\partial B_k^c}{\partial x^j} + \left\{ \begin{matrix} c \\ ab \end{matrix} \right\} B_j^a B_k^b - \left\{ \begin{matrix} k \\ ji \end{matrix} \right\} B_i^c \quad (\equiv \nabla_j B_k^c)$$

is called the Euler-Schouten curvature tensor (Schouten, 1954). The relationship

between this curvature tensor and the Riemann-Christoffel curvature tensor R_{hklj} is given by

$$R_{hklj} = H_{ik}^a H_{jla} - H_{il}^a H_{kja} \quad (H_{jia} = (\nabla_j B_a^i) g_{mi}, \quad B_a^i = g^{im} B_m^a g_{ba}).$$

Then, if $R_{hklj} = 0$ is called *locally flat condition*, $H_{ij}^a = 0$ could be called *globally flat condition*. The possibilities of these conditions are as follows:

1. If $H_{ij}^a = 0$, $R_{hklj} = 0$
2. Even if $R_{hklj} = 0$, $H_{ij}^a = 0$ is not necessarily satisfied.
3. Even if $R_{hklj} \neq 0$, $H_{ij}^a \neq 0$ is not necessarily satisfied.

If there are *perceptually* or *globally* flat planes not only in the simultaneous illusions but also in the figural after-effects, these situations should be defined by $H_{ij}^a = 0$. However, H_{ij}^a cannot be obtained explicitly. Therefore, the authors firstly tried to describe the simultaneous illusion by $R_{hklj} = 0$ and the figural after-effect by $R_{hklj} \neq 0$, because both the formulations could involve $H_{ij}^a = 0$. In Section 2.3, $R_{hklj} \neq 0$ was related to another displacement effect, where a plane appears slightly before or behind the plane. This effect could not be described within two-dimensional plane, which was deduced from the incompatibility condition with respect to distortion tensor.

The model simulation on the basis of the accumulated effects of concentric circles (Section 7) supported also a Riemannian model of *bent line* illusions (Yamanoi et al., 1981). Thus, the present model in terms of no *depth effect* could be responsible for various illusions in concentric circle situation such as the Delboeuf illusion, the figural after-effect for small inspection time and the Orbison illusion.

Imperfection of the present model is that displacement effect becomes a monotone function of the size ratio of the TC to the SC. A better fitting to the present data might be obtained by a confocal transformation of the metric tensor:

$$\bar{g}_{ij} = \frac{1}{\sigma^2} g_{ij}.$$

Then, approximated solutions of $\bar{\phi}(r)$ with $\bar{R}_{hklj} = 0$ are shown in Fig. 8.1. Because

$$\int_{r=r_1}^{r=r_2} ds = 2\pi r_1 \bar{\phi}(\sigma),$$

σ may describe the unit length of the perceived stimulus field. Suppose that this parameter could be psychologically translated into the light threshold and be affected only by stimulus configuration and stimulus intensity, we could assume that

$$\sigma(r) = A_1 \log \frac{r}{r_0 I_c},$$

where r_0 is a correction term with respect to the unit of a distance r and I_c is the

¹¹ The value of I_c for the overestimation of inner circles was set to be smaller than that for the underestimation of outer circles, because the light threshold outside a circle is higher than that inside the circle (Nozawa, 1956, 1958).

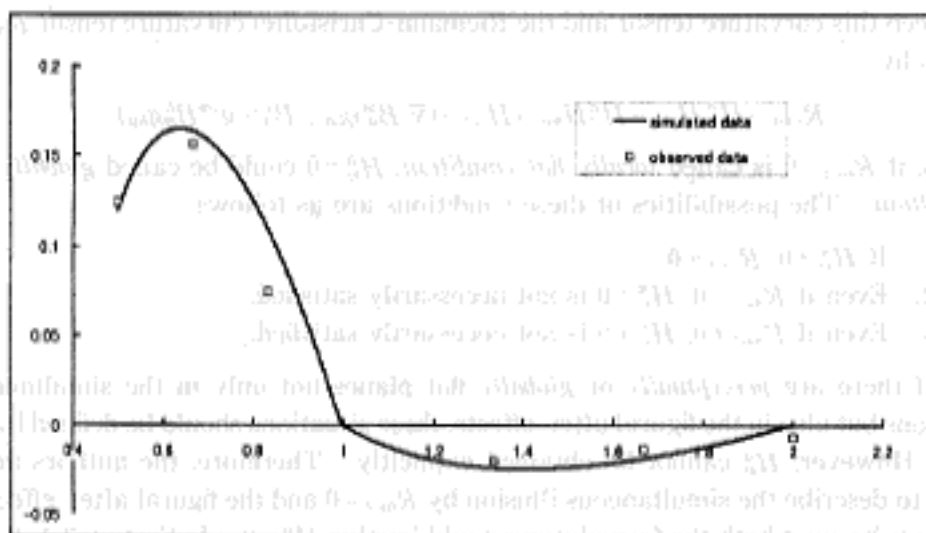


Fig. 8.1 Improved displacement effect on the basis of $\phi(r)$ with $\bar{R}_{ave}=0$ (see Section 8 for the model description).

stimulus intensity. Solid lines in Fig. 8.1 depict numerical solutions of $\bar{R}_{ave}=0$ with $r_u=15$ (mm), $I_c=1.5$ and $r_u=30$ (mm), $I_c=3.3$ for overestimation of inner circles and underestimation of outer circles⁹⁾, respectively, in comparison with the displacement effect observed only for one male subject. Although Fig. 8.1 demonstrates a good choice of σ , its strict specification should be completed by further research.

Acknowledgment

This research was partly supported by a research project of Hokkai Gakuen Hi-Tech Research Center.

REFERENCES

- Blakemore, C., Carpenter, R.H.S. & Georgeson, M.A. (1970). Lateral inhibition between orientation detectors in the human visual system. *Nature*, **228**, 37-39.
- Brown, W.R.J. & MacAdam, D.L. (1949). Visual sensitivities to combined chromaticity and luminance differences. *Journal of the Optical Society of America*, **39**, No. 10, 808-834.
- Caelli, T. (1977). Psychological interpretations and experimental evidence for the LTG/NP theory of perception. *Cahiers de Psychologie*, **20**, 107-134.
- Caelli, T., Hoffman, W. & Lindman, H. (1978). Subjective Lorentz transformations and the perception of motion. *Journal of the Optical Society of America*, **68**, No. 3, 402-411.
- Eschenburg, J.-H. (1980). Is binocular visual space constantly curved? *Journal of Mathematical Biology*, **9**, 3-22.
- Foster, D.H. (1975). Visual apparent motion and some preferred paths in the rotation group $SO(3)$. *Biological Cybernetics*, **18**, 81-89.
- Ganz, L. (1966). Mechanism of the figural aftereffects. *Psychological Review*, **73**, No. 2, 128-150.
- Gillam, B. (1980). Geometrical illusions. *Scientific American*, **242**, 86-95.
- Gregory, R.L. (1968). Visual illusions. *Scientific American*, **219**, 66-76.

- Hoffman, D.D. (1983). The interpretation of visual illusions. *Scientific American*, **249**, No. 6, 137-144.
- Hoffman, W.C. (1971). Visual illusions of angle as an application of Lie transformation groups. *SIAM Review*, **13**, No. 2, 169-184.
- Hubel, D.H. & Livingstone, M.S. (1987). Segregation of form, color, and stereopsis in primate 18. *Journal of Neuroscience*, **7**, 3378-3415.
- Humphrey, D.I.A. & Morgan, M.J. (1965). Constancy and the geometric illusions. *Nature*, **206**, 744-745.
- Ichikawa, S. (1982). Verbal and visual recall span curves between 1 ms and 1 min. *Psychological Research*, **44**, 209-281.
- Ikeda, H. (1951). Zukei zanko ni kansuru kenkyu (Studies in figural after-effects). Tokyo Bunrika University Dissertation (in Japanese, unpublished).
- Ikeda, H. & Obonai, T. (1955). Studies in figural after-effects (IV) — The contrast-confluence illusion of concentric circles and the figural after-effect —. *Japanese Psychological Research*, **2**, 17-23.
- Indow, T. (1974). On geometry of frameless binocular perceptual space. *Psychologia*, **17**, 50-63.
- Indow, T. (1979). Alleys in visual space. *Journal of Mathematical Psychology*, **19**, 221-258.
- Indow, T. (1982). An approach to geometry of visual space with no a priori mapping functions: Multidimensional mapping according to Riemannian metrics. *Journal of Mathematical Psychology*, **26**, 204-236.
- Jain, A.K. (1972). Color distance and geodesics in color 3 space. *Journal of the Optical Society of America*, **62**, No. 11, 1287-1291.
- Kawabata, N. (1976). Mathematical analysis of the visual illusion. *IEEE Transactions on Systems, Man, and Cybernetics*, **SMC-6**, No. 12, 818-824.
- Kogiso, I. Unpublished data.
- Köhler, W. & Wallach, H. (1944). Figural after-effects. An investigation of visual processes. *Proceedings of the American Philosophical Society*, **88**, 269-357.
- Langwitz, D. (1965). *Differential and Riemannian Geometry*. Translated by F. Steinhardt. Academic Press, Inc. (London) Ltd.
- Levi-Civita, T. (1917). Nozioni di parallelismo in una varietà qualunque e conseguente specificazione geometrica della curvatura Riemannia. *Rend. Palermo*, **42**, 173-205.
- Luneburg, R.K. (1947). *Mathematical analysis of binocular vision*. Princeton, N.J.: Princeton Univ. Press.
- MacLeod, D.I.A., Virsu, V. & Carpenter, R.H.S. (1974). On mathematical illusions. *Perception & Psychophysics*, **16**, 417-418.
- Nowakowska, M. (1983). Dynamics of perception: some new models. *International Journal of Man-Machine Studies*, **18**, 175-197.
- Nozawa, S. (1956). An experimental study on figural after-effect by the measurement of field strength I. *Japanese Psychological Research*, **3**, 15-24.
- Nozawa, S. (1958). An experimental study on figural after-effect by the measurement of field strength II. *Japanese Psychological Research*, **5**, 22-27.
- Ogasawara, J. (1952). Doshin en no hen i koka ni tsuite (Displacement-effect of concentric circles). *Japanese Journal of Psychology*, **22**, 224-234 (in Japanese).
- Orbison, W.D. (1939). Shape as a function of the vector field. *American Journal of Psychology*, **52**, 31-45.
- Oyama, T. (1953). Zukei zanko no jikkenteki kenkyu (I) — Jikanteki yoin ni tsuite — (Experimental studies of figural after-effects: I. Temporal factors). *Japanese Journal of Psychology*, **23**, 230-245 (in Japanese).
- Oyama, T. (1954). Zukei zanko no jikkenteki kenkyu (II) — Kukanteki yoin ni tsuite — (Experimental studies of figural after-effects: II. Spatial factors). *Japanese Journal of Psychology*, **25**, 195-206 (in Japanese).
- Oyama, T. (1956). Temporal and spatial factors in figural after-effects. *Japanese Psychological Research*, **3**, 25-36.
- Oyama, T. (1977). Feature analysers, optical illusions, and figural aftereffects. *Perception*, **6**, 401-406.

- Resnikoff, H.L. (1978). Differential geometry and color perception. *Journal of Mathematical Biology*, **1**, 97-131.
- Robinson, J.O. (1968). Retinal inhibition in visual distortion. *British Journal of Psychology*, **60**, 29-36.
- Sagara, M. & Oyama, T. (1957). Experimental studies on figural after-effects in Japan. *Psychological Bulletin*, **54**, No. 4, 327-338.
- Saito, H., Yukie, M., Tanaka, K., Hikosaka, K., Fukuda, Y. & Iwai, E. (1986). Integration of direction signals of image motion in the superior temporal sulcus of the Macaque monkey. *Journal of Neuroscience*, **6**, No. 1, 145-157.
- Schouten, J.A. (1954). *Ricci-calculus*. Berlin/Göttingen/Heidelberg: Springer-Verlag.
- Smith, D.A. (1978). A descriptive model for perception of optical illusions. *Journal of Mathematical Psychology*, **22**, 64-85.
- Toyama, K. & Kozasa, T. (1982). Responses of Clare-Bishop neurons to three dimensional movement of a light stimulus. *Vision Research*, **22**, 571-574.
- Von Schelling, H. (1956). Concept of distance in affine geometry and its applications in theories of vision. *Journal of the Optical Society of America*, **46**, No. 5, 309-315.
- Walker, E.H. (1973). A mathematical theory of optical illusions and figural aftereffects. *Perception & Psychophysics*, **13**, 467-486.
- Walker, E.H. (1974). On spurious illusions. *Perception & Psychophysics*, **16**, 419-425.
- Watson, A. (1978). A Riemann geometric explanation of the visual illusions and figural after-effects. In E.L.J. Leewenberg & H.F.J.M. Buffart (Eds.), *Formal Theories of Visual Perception* (pp. 139-178). Chichester/New York/Brisbane/Toronto: John Wiley & Sons Ltd.
- Yamanoi, T., Yamazaki, T. & Kawaguchi, M. (1981). On the interpretation of some visual illusions by a geometrical model of Riemannian spaces. *Behaviormetrika*, **10**, 77-85.
- Yamanoi, T., Kudo, T., Yamazaki, T. & Kawaguchi, M. (1982). On the interpretation of some visual illusions by a geometrical model of Minkowski space. *TENSOR*, **37**, 257-262.
- Yamanoi, T. (1998). Unpublished data.
- Yamazaki, T. (1987). Non-Riemannian approach to geometry of visual space: An application of affinely connected geometry to visual alleys and horopter. *Journal of Mathematical Psychology*, **31**, No. 3, 270-298.
- Yamazaki, T. (1990). Sakushi gensho ni chakumokushita shikaku joho shori moderu — Doshin en sakushi no teiryoteki hyogen — (A visual information processing model with reference to visual illusions — A quantitative description for contrast-confluence illusion of concentric circles —). *Proceedings of the 5th Symposium on Biological and Physiological Engineering*, 245-248 (in Japanese).
- Yamazaki, T. (1991). Sakushi gensho ni chakumokushita shikaku joho shori moderu — Doshin en sakushi ni okeru zukei zanko heno kakucho — (A visual information processing model of visual illusions — An application to the figural after-effects in the illusion of concentric circles —). *IEICE (The Institute of Electronics, Information and Communication Engineers) Technical Report*, **A191-38/PRU91-41**, 67-73 (in Japanese).

(Received April 1998, Revised September 1998)